

N O T I C E

THIS DOCUMENT HAS BEEN REPRODUCED FROM
MICROFICHE. ALTHOUGH IT IS RECOGNIZED THAT
CERTAIN PORTIONS ARE ILLEGIBLE, IT IS BEING RELEASED
IN THE INTEREST OF MAKING AVAILABLE AS MUCH
INFORMATION AS POSSIBLE

GRADIO: PROJECT PROPOSAL FOR SATELLITE GRADIOMETRY

G. Balmino, F. Barlier, A. Bernard, C. Bouzat, G. Rivière, J. Runavot

(NASA-TM-76796) GRADIO: PROJECT PROPOSAL
FOR SATELLITE GRADIOMETRY (National
Aeronautics and Space Administration) 55 p
HC A04/MF A01 CSCI 08B

N82-20606

Unclas
09405

G3/43

Translation of "GRADIO: Gradiométrie par satellite -- Projet
projet", CENTRE NATIONAL D'ETUDES SPATIALES, Centre Spatiale de Toulouse,
Toulouse, France, Report 244 PRT/AMP/AP, September 8, 1981, pp. 1-51.



1. Report No. NASA TM-76796	2. Government Accession No.	3. Recipient's Catalog No.	
4. Title and Subtitle GRADIO: PROJECT PROPOSAL FOR SATELLITE GRADIOMETRY		5. Report Date December 1981	6. Performing Organization Code
		8. Performing Organization Report No.	10. Work Unit No.
7. Author(s) J. J. Runavot, et al., Centre National d'Etudes Spatiales (France)		11. Contract or Grant No. NASW-3541	
		13. Type of Report and Period Covered Translation	
9. Performing Organization Name and Address Leo Kanner Associates Redwood City, California 94063		14. Sponsoring Agency Code	
		12. Sponsoring Agency Name and Address National Aeronautics and Space Administration, Washington, D.C. 20546	
15. Supplementary Notes Translation of "GRADIO: Gradiométrie par satellite -- Proposition de projet", CENTRE NATIONAL D'ETUDES SPATIALES, Centre Spatiale de Toulouse, Toulouse, France, Report 244 PRT/AMP/AP, September 8, 1981, pp. 1-51.			
16. Abstract A gradiometric approach, rather than the more complicated satellite-to-satellite tracking, is proposed for studying anomalies in the gravitational fields of the earth and, possibly, other telluric bodies. The first analyses of a gradiometer based on four of ONERA's CACTUS or SUPERCACTUS accelerometers are summarized. It is shown that the obstacles to achieving the required accuracy are not insuperable. The device will be carried in a 1000 kg lens-shaped satellite in a heliosynchronous orbit 200-300 km in altitude. The first launching is planned for the end of 1987.			
17. Key Words (Selected by Author(s))		18. Distribution Statement U.S. GOVERNMENT AGENCIES ONLY	
19. Security Classif. (of this report) Unclassified	20. Security Classif. (of this page) Unclassified	21. No. of Pages	22.

OUTLINE OF DOCUMENT

	PAGE
0. Introduction	1
1. Scientific Objectives	3
1.1 Knowledge of the Earth's Field	3
1.2 In Planetology	11
1.3 Other Applications of the Technique	13
2. Instrumentation	14
2.1 The CACTUS and SUPERCACTUS Accelerometers	14
2.2 Principle of the Gradiometer	20
3. The Terrestrial Mission	31
3.1 Technical Analysis of the Mission	31
3.2 Preliminary Design of the Vehicle	39
3.3 Ground Segment	44
3.4 Development Plan	45
3.5 Operation	47
4. Conclusion	50
References	52

GRADIO: PROJECT PROPOSAL FOR SATELLITE GRADIOMETRY

G. Balmino
Bureau Gravim. Inter.

F. Barlier
CERGA

A. Bernard
ONERA

C. Bouzat, G. Riviere, and J.J. Runavot
CNES

Introduction

3*

Knowledge of a body's gravitational field and of its anomalies is a boundary constraint for any physical model of its structure and the behavior of its small deformations. Such knowledge has now become indispensable to other disciplines contributing to the study of the body: seismology, magnetism, topography, etc.

The techniques that have been developed up to now and the methods used to determine the parameters representing spatial variations, or even space-time variations in the field, have produced models of varying accuracy and resolution, not only for the earth, but for other telluric planets and the moon. They permit comparative structural studies, whose impact on the understanding of the geophysical phenomena characteristic of our planet has been great. However, even though these models appear sophisticated to the general public, they are still insufficient to correctly interpret phenomena that affect our planet and certain others in the solar system. Probably one of the most important of such phenomena is the manner in which the variations in gravity, among other geophysical quantities, are linked to the plate tectonics and earthquakes. In order

*Numbers in the margin indicate pagination in the foreign text.

to understand and build models of such phenomena, an understanding that is at once general, detailed, and precise of the anomalies in the various existing fields, particularly in the gravitational field, is necessary.

The only way to achieve a general knowledge and, later, to monitor the time variations in the active zones, involves use of outer space. For terrestrial applications, the presence of the atmosphere necessitates launching satellites whose perturbations are then analyzed or which carry instruments that directly measure variations in the field at an altitude at which the effects to be detected are already very weak. Today, the space techniques are therefore complemented by the use of gravity measurements on the ground (or even in the sea) and by altimetric measurements of the form of the privileged equipotential surface forming the geoid in its oceanic sections. In the oceanic regions, the needs of geophysical studies could, if necessary, be met by the joint usage of the overall information learned through analyzing satellite orbits and of altimetric data. In contrast, the knowledge of anomalies at medium scale, and even more so at high resolution, is imprecise in continental regions (with the exception of western Europe and part of North America) because of poor coverage (often non-existent) and of low accuracy in the measurements of gravity. No improvement can be hoped for in this situation, at least as far as the models available to the international community are concerned.

4

We therefore must look for another method besides altimetry that has equivalent resolution and accuracy, i.e. approximately 1 mgal ($= 10^{-5}$ m/sec²) of accuracy for mean values in 100 x 100 km regions.

There essentially exist two space techniques to achieve these goals, satellite-to-satellite tracking and gradiometry.

Satellite-to-satellite tracking has already undergone study in France (Project Diabolo), Europe (Project Slalom), and the United States (Project Gravsat). This method, based on the analysis of the relative motion of at least two satellites, is certainly very complicated and costly. Its feasibility has not yet been proved. On the other hand, gradiometry is conceptually a simpler method (only one satellite), but it has come up against difficulties that seem to put the necessary accuracy outside our grasp. However, the success of space accelerometry and ONERA's recent research have both indicated a way to overcome these obstacles. The first studies and experimentation carried out by ONERA and CNES are very encouraging and call for a much deeper investigation of the mission and system. In the United States, the development of space gradiometry is linked to the use of ground technologies which carry with them heavy penalties when used in outer space. On the contrary, we are proposing here to start off directly from a preexisting space technology: the CACTUS accelerometer built by ONERA and launched by CNES on board the CASTOR satellite in 1975. The situation is therefore favorable for meeting current, attainable scientific objectives.

1. Scientific Objectives

/5

1.1 Knowledge of the Earth's Field

A more and more detailed global knowledge of the earth's gravitational field is necessary for several purposes:

-- Improvement in reconstructing and extrapolating the trajectories of artificial satellites for practical purposes (navigation, precise positioning by quasi-geometric methods -- dynamic or short arcs) and scientific ones, such as analysis of residual perturbing effects on the trajectories for the study, e.g., earth and oceanic tides; determination of polar motion by methods using radio measurements (Doppler or laser); reduction of altimetric measurements.

Fig. 1

GRIM3CS4 1981 GEOID
A=6378.140 KM; F=1./298.257; GM=398600.5
CH.REIGER,G.BALMINO,B.MOYNOT,H.MUELLER



ORIGINAL PAGE
OF POOR QUALITY

-- Use of altimetric data, not only in geodesy, where this information is employed to define a mean reference surface close to the geoid (and in certain cases equal to it), but also in space oceanographics, provided that this mean surface can be exactly distinguished from the geoid and its temporal variations studied.

In geophysics, at various scales. Figure 1 (GRIM 3 Geoid) shows a recently-made chart of the earth's overall field as determined by analyzing the perturbations of geodetic satellites (observed between 1960 and 1970) and by comparing them with surface information: gravitational anomalies and altimetric heights of the geoid. This model, the third of its type in Europe, is the product of Franco-German cooperation. It is representative of the long and medium wavelengths in the gravitational field ($\lambda/2 \geq 500$ km), as the geoid represented here shows, and corresponds to the harmonics of potential up to an order and degree of thirty-six. The modulations in the geoid (or associated gravitational anomalies) in relation to a reference ellipse express the divergence between the figure and the earth if the earth was in hydrostatic equilibrium. They are directly linked to lateral heterogeneities in internal density. The goal of interpreting the anomalies is to determine the nature of the internal constraints associated with the variations in density, for example, to see whether the earth is sufficiently rigid at the depths studied to behave in an elastic fashion or whether, if it has a more plastic behavior, a dynamic support is necessary (by means of convective motion).

The large-scale undulations in the geoid ($\lambda/2 > 1500$ km) do not show any evident correlation with the topography, whether continental or oceanic. This suggests that they reflect anomalies in deep density, located a few hundred kilometers down in the mantle, or even more. Such anomalies would be related to convection cells within the mantle, proposed as the motive forces of the observed movement in the tectonic plates.

/7

FIG. 2

GEOID DIFFERENCES
GRIM3 CS4 - GEM 10 D



ORIGINAL PAGE IS
OF POOR QUALITY

Despite numerous experiments and various mathematical models, the phenomenon is still poorly understood and suffers from errors which continue to affect the gravitational field in many regions. This is illustrated in figure 2, which depicts the differences between the geoid model cited above and another model (American) that is practically equivalent. The divergence is especially great in the continental zones and is mainly due to the errors tainting the gravitational anomalies used (or to the absence of surface information!).

For shorter spatial scales, the relationship between gravity and topography, especially the marine topography of the great oceanic structures, is remarkable. A striking correlation exists between the geoid's medium wavelength undulations and the tectonics of the ocean floor. Each type of structure, subduction zones, dorsal regions, fracture zones, and continental shelves, has its own particular signature that has been well detected by altimetric techniques. This perfectly expresses the fact that isotasy works at these wavelengths. It is obviously desirable to study such compensation at this scale, and with at least the same accuracy, on the continents, so as to correlate medium undulations with measurements of the crust's horizontal and vertical displacements. This is where space geodesy has a great role to play in the observation of active zones. It can be predicted -- but is impossible to fix a date! -- that the precise determination of the gravitational anomalies in these regions, the measurement of the variations, combined with the continuous measurement of horizontal and vertical displacements, will lead to an understanding of the mechanisms that trigger earthquakes and, perhaps, contribute to predicting them.

The indirect techniques used up to now have practically reached their limits, even when combined with surface information. This is because the problems in the coverage and accuracy of gravimetric measurements cannot be overcome in places where altimetry is indispensable for reasons of accessibility (for

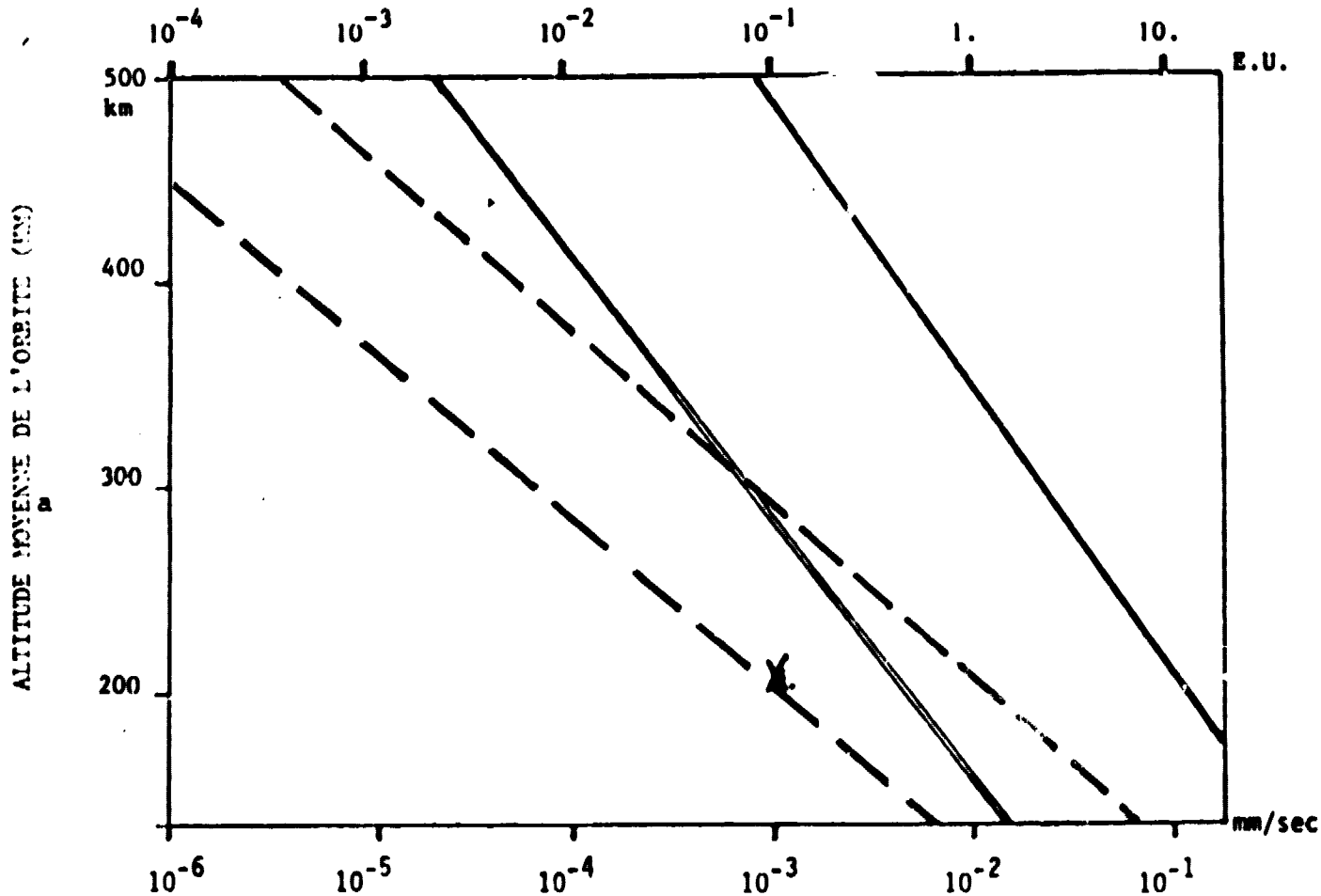
9

example, the Himalayas), politics, and so forth. In addition, even if the earth were covered by oceans, their mean surface, as determined by altimetry, would not coincide with the geoid, and these are the very differences that interest oceanography. We therefore have to come up with an alternative technique. There seem to be only two possibilities at present, satellite-to-satellite tracking (SST) and gradiometry.

The SST technique consists of measuring the radial velocity between two satellites in one of the following configurations: one satellite high (geosynchronous in some cases) and the other low (HL); two satellites in low orbit (LL configuration) and close to one another (50 to 300 km). HL was investigated using GEOS 3 and ATS 6, but confirmation of the technique's validity only occurred once (GEOS 3 was too high, at approximately 800 km). LL was attempted during the Apollo-Soyuz rendezvous, but the test was not conclusive because of the two vessels' complex spurious motion and ionospheric disturbances. In each case, the measurement is interpreted as a difference in gravitational potential between the two objects. The better technique seems to be the LL configuration, and several projects in this direction have been designed: 1) Project Slalom (formerly Diabolo) investigated first by the GRGS alone and then in collaboration with the SFB78 and MBB within the framework of the ESA. This project is based on laser techniques. It uses two Spacelab subsatellites, but the many difficulties linked to the space shuttle seem to be insoluble ... and the mission was very limited, both in space and time. 2) Project Gravsat-A in the USA, consisting of two enormous satellites (6 m long cylinders 1.50 m in diameter, three-axis stabilized, and containing several tons of propellant so as to ensure a one year's life in orbit between 160 and 190 km) and measuring radial velocity by radioelectric technique (approximately 110 GHz). The feasibility of the American project (studied by NASA and the DOD in collaboration with [illegible word]) is far from proven. Even though its estimated cost, which is already very

high, does not seem to be an insuperable obstacle (for the DOD!),
the experiment cannot take place before 1987 at the earliest.

/10



TECHNIQUE	RESOLUTION	
	1° x 1°	1.5° x 1.5°
b PSS/BB	—	—
c GRADIOMETRIE	—	—

Figure 3
Minimum Instrument Accuracy for SST/LL and Gradiometry Techniques
as a Function of Orbital Altitude and for Resolutions of
1° x 1° and 1.5° x 1.5°

- Key: a) Average Orbital Altitude (Km)
b) SST/LL
c) Gradiometry

The gradiometric technique is to measure one or several components of the tensor of second derivatives of gravitational potential in the axes linked to the satellite (there are five independent components). It has never been the object of an experiment in outer space. Under study since the end of the sixties in the USA, gradiometry has led to the design and sometimes the construction and testing (on the ground) of prototypes. There presently exist four American gradiometry projects which, in the presence of gravity, are reported to be capable of achieving a resolution of 0.1 EU (1 Eötvös Unit = 10^{-9} sec⁻², corresponding to a field of 1 mgal = 10^{-3} cm-sec⁻² in 10 km). However, all of these projects suffer from unresolved problems either with the instruments or the environment, and none is yet ready for a space flight. At best, the most recent of them (H.J. Paik's cryogenic gradiometer) might be tested in the space shuttle after 1985 and carried by satellites towards the end of the decade.

In view of the scientific objectives we have enumerated, a resolution of $\lambda/2$ in the 110 to 165 km range ($1^\circ \times 1^\circ$ and $1.5^\circ \times 1.5^\circ$, respectively) could be fixed. An accuracy in reconstructing gravitational anomalies at this scale on the order of one milligal could likewise be decided upon. We can then determine the altitude of the satellite or satellites and the accuracy of the instruments necessary to attain these objectives. Figure 3 summarizes the conclusions of an analytic study founded on an extrapolation to short wavelengths of the orders of magnitude of anomalies in potential for both techniques, SST/LL and gradiometry.

As far as gradiometry is concerned, the reader can therefore bear in mind the compromise given in the following table:

Table 1
Precision of Gradiometric Measurement (EU) as a Function of
Altitude for the Two Resolutions Given

Altitude km Réolution	200	250	300	350	400
1° x 1°	0.10	0.025	0.006	0.002	0.0004
1°5x1°5	0.40	0.20	0.075	0.030	0.015

We shall see in the following chapters how we can meet such conditions.

/12

1.2 In Planetology

The gravitational field of earth-like planets remains the information of choice for constructing any model, even an elementary one, of internal structure in the absence of direct (seismic) measurements. Comparing both the planets' fields with that of the earth and the structures of large and medium scale anomalies with topographical features and surface tectonics is a way to investigate these bodies' origins and thermal and physio-chemical history.

Mars, outside of the regions whose latitude is less than 55° S, is certainly the best known from this point of view, thanks to the Mariner 9 and Viking 1 and 2 missions and to the orbits with very low periastrons from which we have benefited. The resolution of the detected anomalies is on the order of 500 km. Considering the size of the planet, this is similar to global models of the earth. Gradiometry is probably the only technique that could appreciably improve resolution, if not coverage, given the constraints in possible future missions.

Venus offers more interesting possibilities. This stems from the fact that the only sophisticated mission engaged in this type of study, the Venus Pioneer, did not in fact resolve the anomalies sufficiently except in the neighborhood of the periastron of the orbiter (whose latitude was almost constant), i.e. for a zone at 40° latitude. The only coming mission which might carry enough apparatus to answer questions concerning tectonics and isostasy on Venus is VOIR. However, VOIR, as it is envisioned today, requires that experiments be of long duration due to the observational constraints arising from the planet's slow rotation. Whether a gradiometer can function on a vehicle of the type planned and alongside the other instruments remains to be proved.

Of course, we can contemplate missions to Mercury, but this planet is outside Europe's capabilities in view of launch constraints and the small number of scientific instruments it would be possible to carry on board. At present, the United States is not planning any mission to this planet.

The earth-like body which is scientifically the most interesting from the point of view of origin, evolution, and, why not, future development is our natural satellite. The ESA is studying a very complete mission around the moon called Polo. It has taken up the main themes of the American project LPO, which was abandoned at the end of the seventies for budgetary reasons. One of its objectives is to produce a complete cartography of surface physio-chemistry, magnetism, topographical relief, and gravitational anomalies. For this last subject, the planning is to set up a relay satellite in order to use the SST/HL technique to determine the gravitational field of the hidden side. This approach increases the mission's cost and complexity considerably. It is clear that however one wishes to continue studying this mission, i.e. within the ESA or in direct bilateral cooperation with NASA (which is in the process of redefining a new, ambitious lunar mission for the end of the decade), the

elegant and imposing solution is to place a gradiometer on board the orbiter. The fact that the experiment takes place between 50 and 100 km above the lunar surface means that even here a precision of 1 EU, at most 0.1 EU, is satisfactory, given the expected anomalies.

Finally, and this can be considered an extreme case that is not without interest, a gradiometer could "simply" serve to measure the mass of a body such as an asteroid. For example, an asteroid with a diameter of 200 km and a density of 3 g/cm^3 would produce a gravitational gradient of 8 EU on a gradiometer flying by at an altitude of 500 km, a gradient of 26 EU at 300 km, and so forth. In the first case again, the signal would be 27 EU if the asteroid had a diameter of 300 km. Such measurement would be fundamental during an asteroid flyby mission given the large uncertainty (a factor of two) concerning the density of the materials that make up asteroids.

1.3 Other Applications of the Technique

The basis of a gradiometer's operation lies in determining the relative motion of two (or more) small test masses placed inside cavities, without any material contact with the fixed cavities on board the satellite. Because of this fact, the test masses do not undergo any of the nongravitational surface forces affecting the satellite (atmospheric braking and radiation pressure, for example). The restoring forces, of electrostatic origin, exerted on the test masses to keep them near the center of the cavities therefore make it possible to determine these surface forces. In the mission envisaged (circular polar satellite at around 250 km or lower), the total density of the atmosphere can thus be determined very precisely. Even though knowledge of this value has made great progress since the beginning of the space age, its long-term evolution over different solar cycles is still not well enough known. Exact knowledge of it would be very useful for the kind of satellite reentry envisaged in several programs.

The purpose of the gradiometer is to measure the tensor of the second derivative of the potential of gravitational attraction. The technique is presently developed, particularly in the United States, for high resolution determinations of gravitational potential.

In the foreseeable applications with satellites flying by at 300 km from the earth's surface and 100 km from the moon, for example, the difference between the gravitational attraction at two points 1 m meter away from each other is around 10^{-6} m/sec². This difference is equivalent to 1000 EU. (1 EU = 1 Eötvös Unit = 10^{-9} sec⁻².) A gradient of this magnitude suggests that a gradiometer based on a system of ultrasensitive accelerometers like ONERA's CACTUS [Ultra-sensitive Three-Axis Capacitive Accelerometric Sensor] accelerometer could be built.

So as to pinpoint the present state of the technology and make the report easier, we shall review the description and use of this type of accelerometer before taking up the gradiometer's operating principles.

2.1 The CACTUS and SUPERCACTUS Accelerometer [1 to 7]

2.1.1 History

ONERA specially developed these accelerometers for space applications. Thus, CACTUS made up the payload of the French satellite CASTOR that the CNES developed and launched on May 17, 1975. The data acquired during its 45 month orbital life were analyzed by the Grasse Center for Geodynamic and Astronomic Studies and Research (CERGA). The first scientific studies concerned atmospheric temperature and density based on the braking experienced by the satellite between 270 and 400 km altitude.

While CACTUS's expected accuracy was 10^{-8} m/sec², statistical processing of the data allowed an accuracy of 10^{-10} m/sec² to be achieved.

Thus, it was in particular possible to:

- follow the annual variations in solar radiation pressure;
- measure and construct a model of the earth's albedo;
- measure the acceleration due to the earth's infrared radiation.

Finally, the analyses documented well the thrust the satellite felt from its own thermal radiation, whose anisotropy was due to variations in surface temperature. When the satellite was exposed to the sun, this thrust showed up as an acceleration of 3×10^{-9} m/sec². It went down to zero within a few minutes after the satellite entered the earth's shadow.

SUPERCACTUS is a new, higher resolution version, a preliminary study of which was made on the request of the European Space Agency. Use of this accelerometer should make a satellite for measuring all the various components of terrestrial radiation (Project BIRAMIS) possible.

2.1.2 Description and Model of the Accelerometer

The operating principle of CACTUS accelerometers consists of measuring the force developed by triaxial electrostatic suspension to maintain a spherical inertial mass -- a ball -- in the center of a cage attached to a satellite.

Figure 4 is a schematic representation of this servocontrol:

\vec{F} designates the force coming from the satellite that is exerted on the ball of mass m . (\vec{F} is a binding force.)

\vec{F}_E is the resultant of the nongravitational exterior forces applied to the satellite of mass $M - m$.

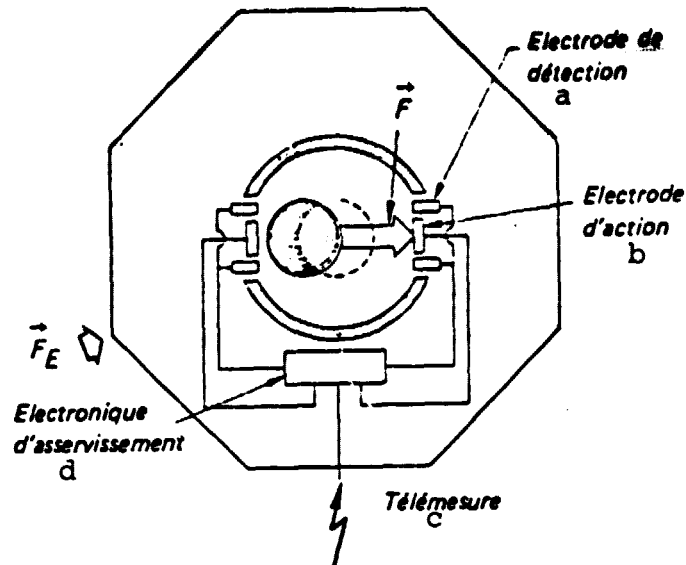


Figure 4
Schematic Diagram of How a Sensitive Axis Functions

Key: a) Detection Electrode c) Telemetry
 b) Action Electrode d) Servocontrol Electronics

Figure 5 specifies the notation used: In the XYZ frame of reference the vectors \vec{r}_G and \vec{r}_B define the positions of the satellite's center of mass and of the center B of the accelerometric ball. A servomechanism keeps the ball at the accelerometer's center O. Consequently, in steady state operation the positional divergence in \vec{OB} is negligible. The ball's position is then defined in relation to the satellite's frame of reference $G(x_s, y_s, z_s)$ by the constant vector \vec{GO} . Using \vec{g}_G and \vec{g}_B to represent the gravitational acceleration at G and B, the equations of motion in the fixed reference system for these two points is written:

/17

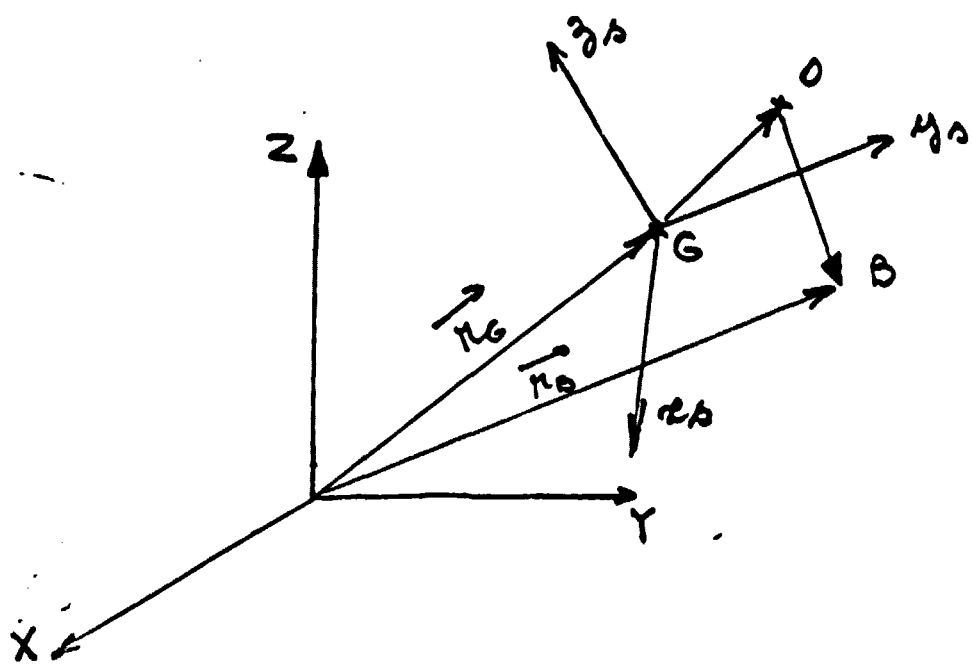


Figure 5

Notation:

- X Y Z: fixed reference system
- $x_s y_s z_s$: satellite's frame of reference
- G: satellite's center of mass
- O: center of accelerometer
- B: center of ball

$$\left\{ \begin{array}{l} \ddot{\vec{r}}_G = \frac{\vec{F}_E - \vec{F}}{M - m} + \vec{g}_G \\ \ddot{\vec{r}}_B = \frac{\vec{F}}{m} + \vec{g}_B \end{array} \right.$$

or for relative motion:

$$(1) \quad \ddot{\vec{GB}} = \ddot{\vec{r}}_B - \ddot{\vec{r}}_G = \frac{\vec{F}}{m} - \frac{\vec{F}_E - \vec{F}}{M - m} + \vec{g}_B - \vec{g}_G$$

To operate the accelerometer and determine \vec{F}_E , it is very desirable to "center" the satellite so that G and O occupy the same position. Since in steady state operation the ball's center B is equal to O, the three points G, O, and B all coincide. Equation (1) is then reduced to:

$$\frac{\vec{F}}{m} = \frac{\vec{F}_E}{M}$$

such that knowledge of \vec{F} makes it possible to directly determine the resultant \vec{F}_E of the nongravitational forces acting on the satellite.

In the general case and when several accelerometers are used, the points G and B are distinct. To take account of acceleration due to the satellite's angular motion, it is then convenient to express equation (1) in the form it takes when projected onto the satellite's frame of reference $x_s y_s z_s$. If the time derivative in this frame of reference is designated by a "°" and $\vec{\Omega}$ used to represent the instantaneous rotational vector, it occurs that:

$$(2) \quad \begin{aligned} \overset{\circ\circ}{\vec{G}}_B + 2\vec{\Omega} \wedge \overset{\circ}{\vec{G}}_B + \overset{\circ}{\vec{\Omega}} \wedge \vec{G}_B + \vec{\Omega} \wedge (\vec{\Omega} \wedge \vec{G}_B) \\ = \frac{\vec{F}}{m} - \frac{\vec{F}_E - \vec{F}}{M - m} + \vec{g}_B - \vec{g}_G \end{aligned}$$

More generally, if n accelerometers are arranged about the satellite, one obtains for each of them:

$$\begin{aligned} \overset{\circ\circ}{\vec{G}}_{B_i} + 2\vec{\Omega} \wedge \overset{\circ}{\vec{G}}_{B_i} + \overset{\circ}{\vec{\Omega}} \wedge \vec{G}_{B_i} + \vec{\Omega} \wedge (\vec{\Omega} \wedge \vec{G}_{B_i}) \\ = \frac{\vec{F}_i}{m_i} - \frac{\vec{F}_E - \sum_{i=1}^n \vec{F}_i}{M - \sum_{i=1}^n m_i} + \vec{g}_{B_i} - \vec{g}_G \end{aligned}$$

Since in steady state operation each is kept in position at the center O_i of the corresponding accelerometer, it occurs that:

$$\vec{G}_{B_i} = \vec{G}_{O_i} \quad \text{and} \quad \overset{\circ\circ}{\vec{G}}_{B_i} = \overset{\circ}{\vec{G}}_{B_i} = \vec{0}$$

such that each accelerometer's output signal \vec{F}_i/m_i is finally expressed as:

$$(3) \quad \boxed{\frac{\vec{F}_i}{m_i} = \vec{g}_G - \vec{g}_{O_i} + \frac{\vec{F}_E - \sum \vec{F}_i}{M - \sum m_i} + \overset{\circ}{\vec{\Omega}} \wedge \vec{G}_{O_i} + \vec{\Omega} \wedge (\vec{\Omega} \wedge \vec{G}_{O_i})}$$

2.2.1 Gradiometry Using Two Accelerators

If the value to be measured is the difference ($\vec{g}_G - \vec{g}_{O_1}$) between the gravitational acceleration at G and O_1 , equation (3) shows that the accelerometer's output signal \vec{F}_i/m_i is not sufficient. It must be freed of the satellite's acceleration

$$\frac{\vec{F}_E - \sum \vec{F}_i}{M - \sum m_i}$$

as well as of the acceleration due to its own angular motion. For that it is natural to turn first to the difference in the measurements made by two accelerometers. Taking equation (3) into account, one can directly obtain:

$$\frac{\vec{F}_1}{m_1} - \frac{\vec{F}_2}{m_2} = \vec{g}_{O_2} - \vec{g}_{O_1} - \overset{\circ}{\Omega} \wedge \vec{O_1 O_2} - \vec{\Omega} \wedge (\vec{\Omega} \wedge \vec{O_1 O_2})$$

The differential measurement eliminates the effect of the external force \vec{F}_E , but it still remains to evaluate the inertial acceleration

$$\overset{\circ}{\Omega} \wedge \vec{O_1 O_2} + \vec{\Omega} \wedge (\vec{\Omega} \wedge \vec{O_1 O_2})$$

For $\|\vec{O_1 O_2}\| = 0.5$ m, an angular velocity Ω_L of 2×10^{-3} rad/sec or an angular acceleration $\overset{\circ}{\Omega}_L$ of 4×10^{-6} rad/sec² along the directions perpendicular to $\vec{O_1 O_2}$ would give rise to an acceleration of 2×10^{-6} m/sec². Such a perturbation is equivalent to the action of a gravity gradient of 4000 EU.

In other words, to obtain 0.1 EU accuracy requires estimation of:

- Ω_{\perp} , with an accuracy of $10^{-10}/2 \Omega_{\perp}$, or, for the example chosen, to the nearest 2.5×10^{-8} rad/sec; and
- $\dot{\Omega}_{\perp}$ to the nearest 10^{-10} rad/sec².

In practice, this level of accuracy is not attainable with the apparatus used for reconstructing satellite attitude. The gradiometer alone must therefore nullify the effects due to the satellite's angular motion. This requires at least four accelerometers. /20

2.2.2 Gradiometry Using Four Accelerometers

The basic principle consists of defining a particular arrangement such that inertial acceleration can be eliminated when processing the accelerometric measurements. Figure 6 illustrates the arrangement envisioned. The centers O_1, O_2, O_3, O_4 of the four accelerometers are arranged at the vertices of a unit square. The center O of the square does not necessarily coincide with the satellite's center of mass G .

In what follows, the vector equations are written directly in the instrument's frame of reference xyz . $\vec{\Omega}$ and $\dot{\vec{\Omega}}$ describe this reference system's angular motion relative to the fixed one. It is necessary at this stage to make the gravity gradients explicit. By definition the corresponding tensor (T) is symmetric and its trace is zero (the derived field of a potential).

$$(4) \quad [T] = \begin{bmatrix} T_{xx} & T_{xy} & T_{xz} \\ T_{xy} & T_{yy} & T_{yz} \\ T_{xz} & T_{yz} & T_{zz} \end{bmatrix} \quad \text{with} \quad T_{xx} + T_{yy} + T_{zz} = 0$$

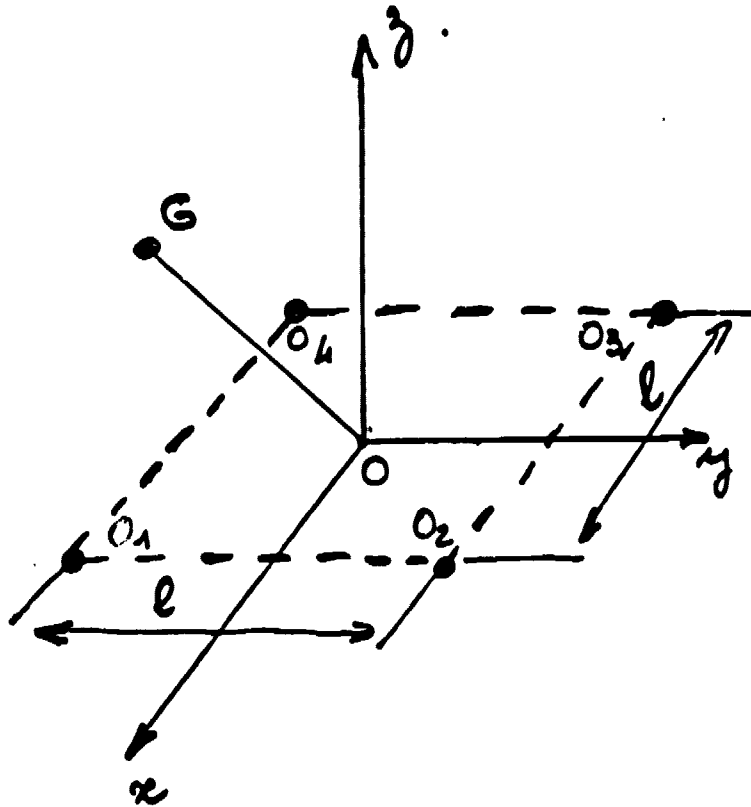


Figure 6
Gradiometry Using Four Accelerometers: Arrangement Adopted

x, y, z: the gradiometer platform's frame of reference
 O: center of the platform
 O_i : center of accelerometer i
 G: satellite's center of mass
 $\vec{\Omega}, \dot{\vec{\Omega}}$: platform's angular motion

In all, therefore, (T) only includes five independent elements.

In considering the acceleration at the center O of the square constituted by the gradiometer, it happens that:

$$(5) \quad \vec{g}_{O_i} = \vec{g}_O + [T] \vec{OO}_i$$

and it is possible to distinguish two terms in equation (3) of the measurement produced by each accelerometer:

$$(6) \quad \frac{\vec{F}_i}{m_i} = \vec{F} + \vec{F}_i$$

\vec{F} is an acceleration acting in common mode on all four accelerometers:

$$(7) \quad \vec{F} = \vec{g}_G - \vec{g}_0 + \frac{\vec{F}_G - \sum \vec{F}_i}{M - \sum m_i} + \overset{\circ}{\Omega} \wedge \vec{G}0 + \vec{\Omega} \wedge (\vec{\Omega} \wedge \vec{G}0)$$

\vec{F}_i is an acceleration directly proportional to the separation $\vec{O}O_i$:

$$(8) \quad \vec{F}_i = [\tau] \vec{O}O_i + \overset{\circ}{\Omega} \wedge \vec{O}O_i + \vec{\Omega} \wedge (\vec{\Omega} \wedge \vec{O}O_i)$$

The square arrangement results in:

$$\vec{O}O_1 = - \vec{O}O_3$$

and

$$\vec{O}O_2 = - \vec{O}O_4$$

which makes:

$$(9) \quad \vec{F}_1 = - \vec{F}_3 \quad \text{and} \quad \vec{F}_2 = - \vec{F}_4$$

Then, considering the body of measurements supplied by the four accelerometers:

$$(10) \quad \begin{aligned} \vec{a} &= \vec{F} + \vec{F}_i \\ \vec{F} &= \frac{1}{4} \sum_{i=1}^4 \frac{\vec{F}_i}{m_i} \end{aligned} \quad \text{i varying from 1 to 4, one obtains:}$$

$$(11) \quad \left\{ \begin{aligned} \vec{F}_1 &= -\vec{F}_3 = \frac{1}{2} \left[\frac{\vec{F}_1}{m_1} - \frac{\vec{F}_3}{m_3} \right] \\ \vec{F}_2 &= -\vec{F}_4 = \frac{1}{2} \left[\frac{\vec{F}_2}{m_2} - \frac{\vec{F}_4}{m_4} \right] \end{aligned} \right.$$

Equation (10) makes it possible to operate a system working together as an accelerometer. Equations (11) are the only ones usable for the gradiometer and lead to a total of six scalar equations, which are easily written out by taking account of (8):

with

$$\begin{aligned} \vec{\Omega} &= [\Omega_x \quad \Omega_y \quad \Omega_z]^T \\ \dot{\vec{\Omega}} &= [\dot{\Omega}_x \quad \dot{\Omega}_y \quad \dot{\Omega}_z]^T \end{aligned}$$

one obtains:

$$(12) \left\{ \begin{array}{l} \left[\begin{array}{l} T_{xx} - T_{xy} + \dot{\Omega}_z - \Omega_x \Omega_y - \Omega_y^2 - \Omega_z^2 \\ T_{xy} - T_{yy} + \dot{\Omega}_z + \Omega_x^2 + \Omega_x \Omega_y + \Omega_z^2 \\ T_{xz} - T_{yz} - \dot{\Omega}_x - \dot{\Omega}_y + \Omega_x \Omega_z - \Omega_y \Omega_z \end{array} \right] = \frac{1}{\ell} \left(\frac{\vec{F}_1}{m_1} - \frac{\vec{F}_3}{m_3} \right) \\ \left[\begin{array}{l} T_{xx} + T_{xy} - \dot{\Omega}_z + \Omega_x \Omega_y - \Omega_y^2 - \Omega_z^2 \\ T_{xy} + T_{yy} + \dot{\Omega}_z - \Omega_x^2 + \Omega_x \Omega_y - \Omega_z^2 \\ T_{xz} + T_{yz} + \dot{\Omega}_x - \dot{\Omega}_y + \Omega_x \Omega_z + \Omega_y \Omega_z \end{array} \right] = \frac{1}{\ell} \left(\frac{\vec{F}_2}{m_2} - \frac{\vec{F}_4}{m_4} \right) \end{array} \right.$$

This system includes 11 unknowns ($\vec{\Omega}$, $\dot{\vec{\Omega}}$, (T)) and is only linear if the direction of the instantaneous vector of rotation is known. It is therefore desirable to impose this direction in a way that minimizes the errors due to the uncertainties in $\vec{\Omega}$ and $\dot{\vec{\Omega}}$. For that, it has proved to be particularly interesting to orient the satellite's angular velocity $\vec{\Omega}$ along the z-axis perpendicular to the plane of the square $O_1O_2O_3O_4$. Thus:

$$(13) \quad \vec{\Omega} = [0 \ 0 \ \Omega_z]^T$$

which supposes in addition that:

$$(14) \quad \dot{\vec{\Omega}} = [0 \ 0 \ \dot{\Omega}_z]^T$$

System 12 now has only seven unknowns:

- Ω_z and $\dot{\Omega}_z$ on the one hand, and
- the five independent elements of tensor (T) on the other.

After eliminating Ω_z and $\dot{\Omega}_z$, it should therefore be possible to obtain four independent equations between the gravity gradients from the six equations in (12).

However, conditions (13) and (14) are never perfectly satisfied, and, in particular, the residual values of $\dot{\Omega}_x$ and $\dot{\Omega}_y$ are directly expressed as errors in the gradients. For accelerations $\dot{\Omega}_x$ and $\dot{\Omega}_y$ of 10^{-10} rad/sec², the error in Txz (or Tyz) is 10^{-10} sec⁻², or 0.1 EU. This leads to restricting the measurements to the components located in the gradiometer's xy-plane. There are only three tensor elements active in this plane (Txx, Txy, and Tyy). After eliminating $\dot{\Omega}_z$ and $\dot{\Omega}_y$, the four equations to retain in system (12) finally make it possible to obtain two relationships containing these three elements. Using $\Delta\Omega_x$ and $\Delta\Omega_y$ to represent the residual values of $\dot{\Omega}_x$ and $\dot{\Omega}_y$, one obtains, after all the calculations:

$$(15) \left\{ \begin{array}{l} \frac{1}{2l} \left[\left(\frac{F_{1x}}{m_1} - \frac{F_{3x}}{m_3} \right) + \left(\frac{F_{2x}}{m_2} - \frac{F_{4x}}{m_4} \right) + \left(\frac{F_{1y}}{m_1} - \frac{F_{3y}}{m_3} \right) - \left(\frac{F_{2y}}{m_2} - \frac{F_{4y}}{m_4} \right) \right] \\ \quad = T_{xx} - T_{yy} + \Delta\Omega_x^2 - \Delta\Omega_y^2 \\ \frac{1}{2l} \left[- \left(\frac{F_{1x}}{m_1} - \frac{F_{3x}}{m_3} \right) + \left(\frac{F_{2x}}{m_2} - \frac{F_{4x}}{m_4} \right) + \left(\frac{F_{1y}}{m_1} - \frac{F_{3y}}{m_3} \right) + \left(\frac{F_{2y}}{m_2} - \frac{F_{4y}}{m_4} \right) \right] \\ \quad = T_{xy} + \Delta\Omega_x \Delta\Omega_y \end{array} \right.$$

The effects due to the angular acceleration $\dot{\Omega}$ are completely eliminated. The residual velocities $\Delta\Omega_x$ and $\Delta\Omega_y$ only intervene in the form of squares or products such that an accuracy of 0.1 EU = 10^{-10} sec⁻² corresponds to the specifications:

$$\Delta\Omega_x \text{ and } \Delta\Omega_y < 10^{-5} \text{ rad/s}$$

The attitude control system has to be able to accommodate this constraint.

2.2.3 Implementing the System and Anticipated Accuracy

When the velocity deviations $\Delta\Omega_x$ and $\Delta\Omega_y$ are zero and the square $O_1O_2O_3O_4$ is perfectly regular, the accuracy is only limited by:

- the satellite's contribution to the gravity gradients T_{xx} , T_{yy} , and T_{xy} , and
- the accuracy of the accelerometers themselves.

The satellite's contribution to the gradients may attain 10 EU, but presents the peculiarity of being practically constant in the gradiometer's xyz reference system (which is connected to the satellite). The satellite's gravitational attraction has to be evaluated in flight. While not attributable to the operating scheme adopted for the gradiometer, it should be taken into account when designing the satellite and analyzing its mission.

As for the accelerometers' accuracy, the error in measurement obtained along a sensitive axis mainly results from three terms. For the x-axis of accelerometer i, the measurement is F_{xi}/m_i and the error is expressed as:

$$(16) \quad \Delta\left(\frac{F_{xi}}{m_i}\right) \approx \Gamma_{0xi} + \frac{\Delta S}{S} \times \frac{F_{xi}}{m_i} + b_{xi}$$

Γ_{0xi} is a bias resulting from spurious forces inside the accelerometer and whose anticipated value in the SUPERCACTUS is 10^{-10} /25 m/sec^2 . For $l = 0.5$ m, this value corresponds to an uncertainty on the order of 0.2 EU. Thus, not only is this effect indistinguishable from the satellite's contribution to the gradients, but, in addition, its value is much smaller.

b_{xi} represents the thermal noise emitted by the electronic servocontrol circuitry. This noise is mostly found in the highest frequencies of the accelerometer's passband and, as a result, can be easily filtered out. Thus, for SUPERCACTUS, the use of a low-pass filter with a 15 sec time constant reduces b_{xi} to 10^{-12} m/sec², or for $l = 0.5$ m, a noise equivalent to approximately 2×10^{-3} EU. This value represents the instrument's thermodynamic limit when the integration time is 15 sec. It is advisable to remember that in spite of the design adopted, the inertial acceleration arising from the satellite's angular motion in reality causes perturbations that are a priori greater than this theoretical limit.

$\frac{\Delta S}{S} \times \frac{F_{xi}}{m_i}$ expresses the error corresponding to the relative uncertainty in the accelerometer's scale factor S . Since the accelerometer's range is too small (less than 10^{-4} m/sec²) to allow it to function on the ground, pre-liftoff determination of its sensitivity S can only be accomplished indirectly. Under these conditions, it is not possible to anticipate an accuracy of better than 10^{-3} for $\Delta S/S$. Thus, in the presence of acceleration F_{xi}/m_i on the order of 10^{-6} m/sec², the value obtained should be:

$\frac{\Delta S}{S} \times \frac{F_{xi}}{m_i} = 10^{-9}$ m/sec², or an uncertainty in the gravitational gradients of about 2 EU (for $l = 0.5$ m).

Even though it is desirable to minimize the value of the acceleration F_{xi}/m_i , equation (3) shows that the limit to consider is fixed by $|\frac{\vec{g}_i}{g_0} - \vec{g}_0|$ whose value is precisely on the order of 10^{-6} m/sec². It should be noted in addition that, among the accelerations endured by the instrument, \vec{F}_E/M corresponds to the amount of atmospheric braking exerted on the satellite, which varies greatly with altitude.

Since the values of the acceleration are only susceptible to being increased, one must try to reduce the error produced by the uncertainty $\Delta S/S$ in the scale factor. Now, gradiometry relies only

/26

on differential measurements. Thus, when the same systematic error in sensitivity taints all the accelerometric measurements, this error transfers directly onto the gradient measurements (for the same reason as an uncertainty in the length l of the sides of the squares does). Attainment of accuracies better than 1 EU (for accelerations of 10^{-6} m/sec²) therefore requires that the accelerometers' scale factors be equalized in flight. Such an operation could be performed by a servocontrol system like the one represented in figure 7.

A calibration device generates a sinusoidal acceleration Γ at pulsance ω in the accelerometers' passband. This acceleration, which can be obtained by rotating a small, unbalanced wheel connected to the gradiometer at constant velocity, for example, is applied in common mode to both accelerometers A_1 and A_2 whose sensitivities S_1 and S_2 are to be equalized. Synchronously demodulating A_1 's and A_2 's output signal at a pulsance ω makes it possible to extract the difference $(\hat{\Gamma}_1 - \hat{\Gamma}_2)$ between the measurements obtained for Γ . The sensitivity S_2 is then adjusted so as to equal S_1 by introducing a modification ΔS_2 proportional to the integral of $(\hat{\Gamma}_1 - \hat{\Gamma}_2)$. This last value remains constant when $S_1 = S_2$.

It is difficult to define beforehand the limit of the accuracy in this feedback control. Values on the order of 10^{-4} to 10^{-5} seem reasonable.

In conclusion, the evaluation of the gradiometer's overall accuracy should be the occasion for a serious parametric study of the instrument, the satellite, and the mission. However, the envisaged operating principles and the orders of magnitude presented indicate that a resolution of better than 0.1 EU in the presence of perturbing accelerations at least equal to 10^{-6} m/sec² is possible.

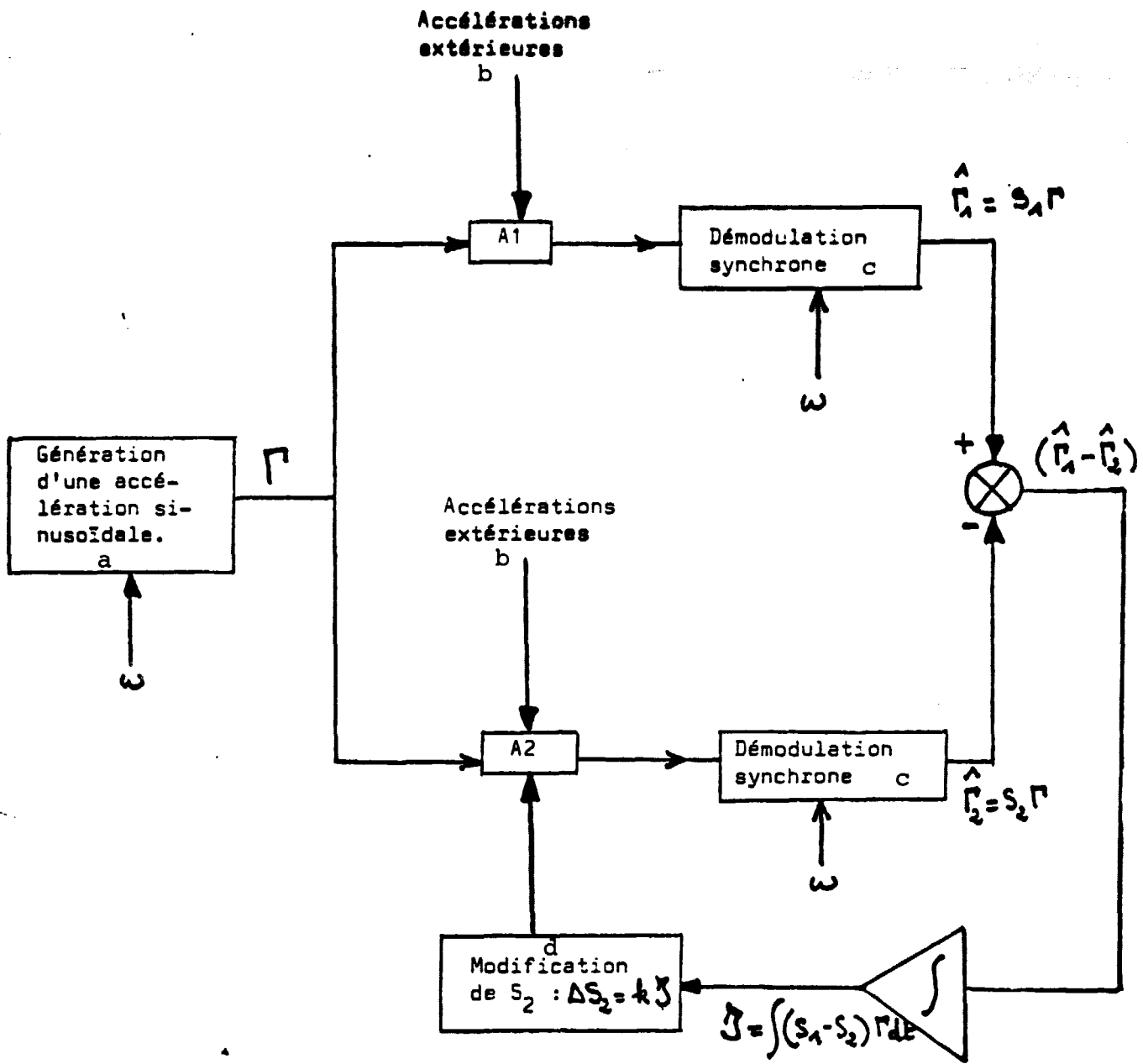


Figure 7
 Servocontrol for Equalizing Scale Factors S_1 and S_2
 of Accelerometers A_1 and A_2

- Key:
- a) Generation of a sinusoidal acceleration
 - b) External Acceleration
 - c) Synchronous demodulation
 - d) Modification of S_2 :

3.1 Technical Analysis of the Mission [8]

3.1.1 Principle of the Mission

To obtain a good representation of the earth's potential with the aid of sufficiently exact measurements of a certain number of components of the tensor of the earth's gravitational gradient.

The measurement of these components is performed by making three-axis differential acceleration measurements with SUPERCACTUS type accelerometers arranged according to a certain geometric configuration.

The basic configuration used is one with accelerometers distributed about a square (figure 8).

Obviously, the earth mission is much trickier than the other planetological ones accessible to the envisaged gradiometer because of the earth's atmosphere and the precision sought (beyond the 36th harmonic).

3.1.2 Main Constraints

- Global coverage of the earth in small enough steps.
- No saturation of any microaccelerometer's output (which would entail the total loss of the information).
- The spurious acceleration terms must be identified with a precision compatible with the resolution sought after, in conformity with table 1.

ORIGINAL PAGE IS
OF POOR QUALITY,

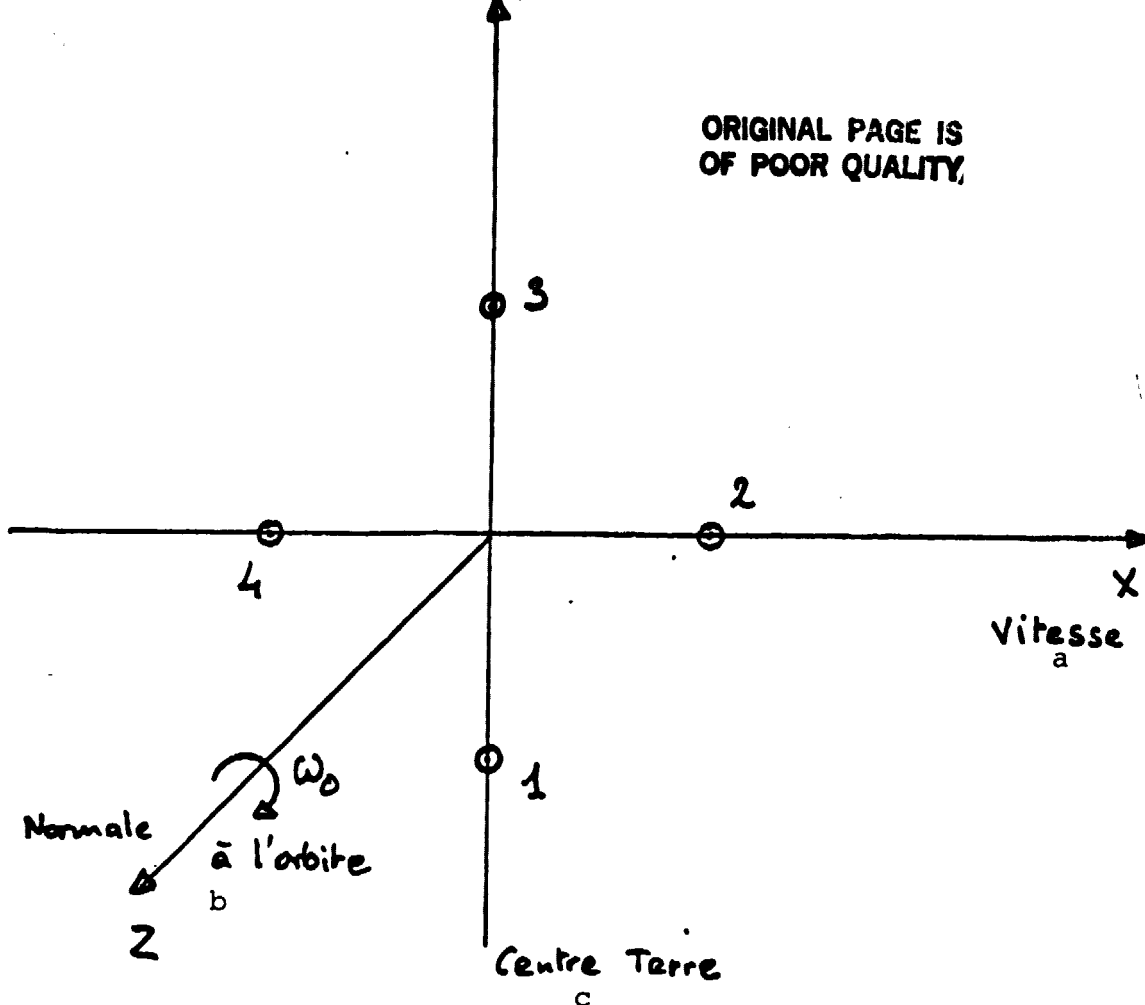


Figure 8
Geometry and Arrangement of an Instrumental Group
Relative to a Local Orbital Frame of Reference

Key: a) velocity
b) normal to the orbit
c) center of the earth

3.1.3 Discussion of Principal Factors

Orbit: Almost total coverage of the earth requires an orbit of high inclination and therefore one that is practically polar. In addition, the opportunities for sending up secondary passenger transports (Viking philosophy) into heliosynchronous orbits during launchings of multimission platforms of the SPOT variety support the choice of such an orbit as the parking orbit. Taking account of the cost in mass of major orbital corrections, a final orbit that is accessible at the end of a reasonable period of time and with a reasonable increase in speed is called for.

We will therefore assume in what follows that we are working in a heliosynchronous or quasi-heliosynchronous orbit. This results in coverage of more than 99% of the earth's surface (99.36% for 96.5°) with two parameters to determine: altitude and local time of node.

/31

Local time of node: The preliminary analysis of the problems of measurement and both attitude and orbital control led to recommending a measurement system composed of floating gyros and suggested the use of ionic engines to partially compensate for atmospheric drag. The attitude and orbital control system will therefore consume significant amounts of energy. The obvious necessity to have a very low A/m (this point is developed in detail below) is the basis for rejecting solar generators that turn or are too large.

/32

To produce enough power with a generator stuck to the vehicle's skin, a major main frame member must point towards the sun. In order to minimize A/m in the direction of the aerodynamic wind, this maximum main frame member must be perpendicular to the normal of the orbit. The sun's direction must be as close as possible to the orbit. In conclusion, the local time of the ascending node has to be 6:00 or 18:00. The choice depends on the primary orbit dictated by the principal passenger (minimization of drift time).

Altitude. This parameter affects:

- The continuous components of acceleration (aerodynamic drag, continuous vehicle rotation, first term of the potential) which threaten to saturate the accelerometer.
- The sensitivity required for isoresolution gradient measurement in anomalies (table 1 and figure 3).
- The quality of coverage in terms of step, time, and redundancy in a short mission (six months or one year). Table 2 presents the principal parameters related to the quality of coverage.

-- The useful lifespan in terms of maintenance within the range of altitudes in which measurement is possible. (The useful lifespan is sharply lower than the lifespan in the traditional sense of the term.)

Table 2
Coverage as a Function of Chosen Orbit

Mean Altitude (km)	Inclination* (o)	Orbital Period* (mn)	Coverage** Resolution (km) in n days
200	96.408	88.395	220 - 24 84 - 48 32 - 95 20 - 190
220	96.477	88.798	280 - 16 90 - 46 16 - 230
240	96.546	89.202	330 - 18 80 - 67 10 - 472
260	96.616	89.607	300 - 19 110 - 37 35 - 112
280	96.687	90.012	64 - 78 6 - 390
300	96.758	90.418	400 - 12 130 - 35 22 - 210

*Calculations made with $R_{\text{mean}} = 6370 \text{ km}$, $GM = 39,8601 \text{ km}^3/\text{sec}^2$, $C_{20} = -1.082628 \times 10^{-3}$, eccentricity held at 0.001.

**According to the case, certain regions might in fact be better covered than the table indicates. The figures therefore give the maximum distance between two traces.

The first analyses carried out showed that above 300 km measurement accuracy is limited by the accuracy in reconstructing the angular velocities that induce the inertial accelerations $\gamma_i = \dot{\Omega} \vec{r} + \Omega^2 \vec{r}$, where

$$\Omega = \begin{vmatrix} 0 & -\omega z & \omega y \\ \omega z & 0 & -\omega x \\ -\omega y & \omega x & 0 \end{vmatrix},$$

that the gradiometer cannot distinguish from the acceleration gradients of the earth's potential.

In addition, taking account of the predictable gradiometer dynamic range, the vertical channel threatens to saturate should the vehicle rotate at the orbital velocity. /34

A preliminary analysis of this point is found in [9].

The simplified system of equations giving the measurements' accuracy is:

$$\Delta (T_{xx} - T_{yy}) < 4\Delta\gamma_m + 4\omega \cdot \Delta\omega$$

$$\Delta T_{xy} < 2\Delta\gamma_m + 2\omega \cdot \Delta\omega$$

where:

-- $\Delta\gamma_m$ is the gradiometer's error in measurement expressed as a function of the measurement field γ_0 : $\Delta\gamma_m = \epsilon\gamma_0$.

-- ω is the residual angular velocity (maximum model).

-- $\Delta\omega$ is the gyro unit's error in reconstructing the angular velocity.

As a first approximation, the values adopted for ω and $\Delta\omega$ are respectively 5×10^{-4} and 2×10^{-4} deg/sec. Starting from there, the choice of measurement field γ_0 and dynamic range $1/\epsilon$ establishes the measurement accuracy in Eötvös units. This leads to the maximum altitude as determined with the aid of figure 3.

For the problem to have a solution, the accelerations acting on each accelerometer and each channel (aerodynamic drag, solar radiation pressure, gravity gradient of the spherical earth, and inertial forces connected with rotation relative to the inertial reference system) must be less than γ_0 .

If the vehicle rotates about the normal to the orbit, the dominant accelerations are:

/35

-- Along the local vertical YY:

Vertical gravitational gradient
Rotation about the normal $\pm \omega z^2$

-- Along the tangent XX:

Horizontal gravitational gradient
Rotation about the normal $\pm \omega z^2$
Atmospheric drag

-- Along the normal ZZ:

Horizontal gravitational gradient
Solar radiation pressure (negligible)

The first evaluations reveal feasibility problems when using a theoretically realistic value for the gradiometer's dynamic range, i.e. $\epsilon = 10^{-5}$.

This suggests the use of an ionic engine to at least partially compensate for atmospheric drag, this XX term being the most critical. The use of such a propulsive system would in any case be necessary to compensate for erosion of the orbit at this altitude (even with the low A/m hoped for), since the range of allowed altitudes for correct measurements is small.

Furthermore, the level of thrust is limited to 10 mN because of the ionic engine's high electrical consumption (375 W for 10 mN).

If T is the drag and F the engine's thrust, it is advisable to ensure that $|F - T|/M < \gamma_0$ in order to have measurements and that $F - T > 0$ along an orbit.

Reconstructing attitude and orbit: The accuracy in reconstructing the attitude is expected to be on the order of a half-degree (effect less than one-tenth EU), and in this situation the control accuracy is not important. /36

As for the orbit, the principal constraint concerns reconstructing the altitude with an accuracy on the order of 10 to 100 meters so as not to introduce too great an error as altitude decreases.

3.1.4 Summary of Preliminary Conclusions

The measurements themselves: The accuracy and dynamic range of the measurements have to be studied more in depth. This particularly concerns:

- the final accuracy in control and reconstruction of angular velocities as a function of the passband;
- the exact value of the gradiometer's dynamic range $1/\epsilon$ (equalization of scale factors, especially) as a function of the passband;

- the spectral nature of the desired information so as to judge its spectral separation from different perturbations.

The orbit: Preferable orbit: 6:00 or 18:00 heliosynchronous orbit with an altitude of between 200 and 300 km. Reconstruction of vertical position: to the nearest 10 to 100 m.

The vehicle should have:

- a minimum A/m perpendicular to the aerodynamic wind,
- a maximum surface area perpendicular to the normal to the orbit;
- an almost constant attitude relative to the local orbital frame of reference: orbital control + rotation at orbital pulsance;
- very low angular velocities (flight control with high damping coefficient, elevated inertia, reduction of perturbations) and the lowest possible pulsance, and measure them with precision;
- a capability to make major orbital changes; /37
- an ability to change attitude for doing calibrations or making complementary measurements;
- provisions for providing the instrument itself with a high degree of mechanical and thermal stability (between the four accelerometers and between the instrument and the vehicle's frame of reference).

3.2 Preliminary Design of the Vehicle

3.2.1 Architecture of the Unit (Figure 9)

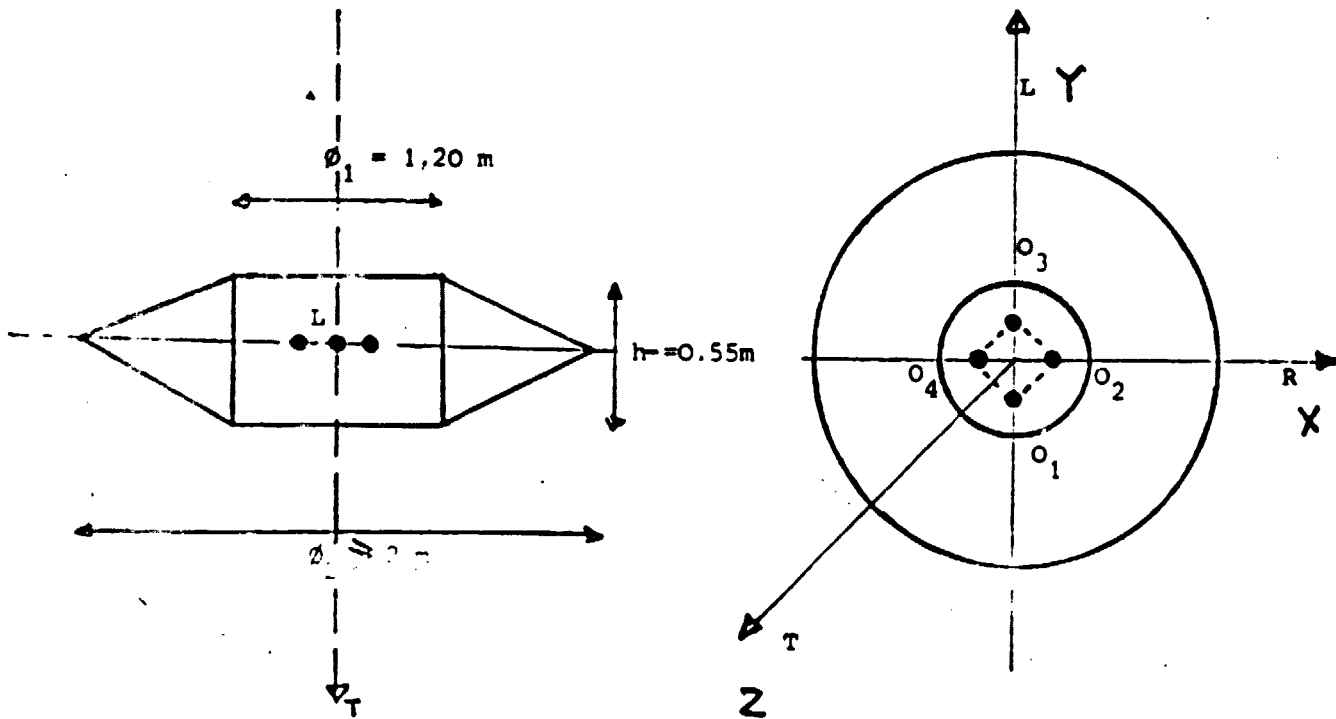


Figure 9

The vehicle's external shape is lenticular (or discoid). It is centered on a cylindrical collar of the standard 1200 diameter joining the SPOT multimission platform to the Ariane (exactly like on the Viking) and has a height of 0.5 to 0.55 m.

The type of control system that governs the vehicle's flight relative to the local orbital reference system allows for a minimum main frame member (less than 1 m^2) facing the aerodynamic wind and a maximum one (greater than 3 m^2) facing the sun.

Considering the Ariane 3's performance in an orbit of the SPOT type (822 km), i.e. 3400 kg, and the predicted maximum mass of 2000 kg

for a satellite using the SPOT multimission platform, we can hope for a mass of around 1000 kg and therefore a ballistic coefficient A/m of 10^{-3} . (Remember that the D5B $\frac{A}{m} = 5.6 \times 10^{-3}$.)

The mass allowance over and above the preliminary tally of mass requirements is enough to plan for an annular ballast of heavy material around the edge to achieve a high level of inertia, greater than several hundred m^2 -kg. This margin of unallocated mass also has to cover the lower braces connected to the central tube and the 1200 diameter adapter. A more detailed analysis has to be made of how the central tube can be arranged to allow for the cohabitation of the instrument and the propulsive system.

/38

3.2.2 Mechanical and Thermal Architecture

The essential points of the structural design concern:

- the braces connecting the peripheral ring and the central tube;
- the connection between the instrument and the central tube (dimensional and directional stability).

On the subject of heat distribution, the vehicle will have the side covered with solar cells continually facing the sun while the opposite side will be in the shade. It is therefore advisable to provide a high degree of thermal coupling between the two sides. In addition, the radial and circumferential gradients have to be minimized (or at least their variation has to be) because they directly affect the bias due to the satellite.

3.2.3 Attitude and Orbital Control System

Normal Mode [9]

The recommended attitude measurement system includes a gyro unit

derived (by simplification) from that of the SPOT and two photocell strip star trackers. The attitude control system should be based on the use of flaps controlled by incremental motors. A set of four flaps that are symmetric in relation to the xz and xy planes and located in a plane parallel to the y-axis will provide three-axis attitude control, particularly since the other perturbing torques are negligible in comparison with the aerodynamic torque.

Orbital control (compensation for drag in order to measure and maintain altitude) will be accomplished with the help of an RIT type ionic engine (manufacturer: MBB) whose thrust can be adjusted between 5 and 10 mN before takeoff.

Its specifications are:

/39

Thrust:	between 5 and 10 mN
I_{sp} :	31,000 NS/kg
Fuel Supply Mass:	11 kg
Engine mass:	4.3 kg
Electrical Consumption:	230 W for 5 mN, 375 W for 10 mN

Future studies will develop a strategy for using this propulsive system that takes its high electrical consumption into account.

Attitude acquisition: The satellite will be placed in an 800 km circular orbit with a random initial attitude and an initial velocity that might reach 12 deg/sec about each axis. Achieving the nominal attitude will therefore require an attitude measurement system.

Attitude acquisition will take place in the following phases:

- reduction of velocity components;
- solar pointing with the aid of a fine solar sensor;
- Commencement of slow spin about the pointed axis; acquisition

of stars by the star tracker and telemetric processing, with evaluation of the satellite's attitude using ephemerides;

-- transition to operational mode by using the star trackers.

During these different phases, the attitude control system will have to produce torques along the three axes with minimal fuel consumption. Considering the relatively low inertias, the torques will not have to be too great.

A cold gas jet system therefore seems appropriate. This is especially true since it would allow attitudinal maneuvers in the 800 km orbit for possible instrument calibrations and could induce the spacecraft to spin or alter its attitude in preparation for orbit changing impulses.

/40

Mass and power tally sheet (outside of the system for changing orbits):

	Acquisition		Normal Mode	
	mass	power	mass	power
Attitude Measurement	21 kg	45 W	21 kg	45 W
Orbital and Attitude Control	(- (6 kg (-	6 W	1 x 16,3 4 kg	375 W 0 W
Propellants	3 kg	--	22 kg	--
Total	73 kg	51 W	73 kg	420 W

Orbit acquisition: The vehicle will have to move from a circular /41 orbit to one with a different plane and altitude. With the exception of proposals involving aerodynamic braking, at least two impulsions will be necessary. Furthermore, the satellite will have to pass through an intermediate drift orbit because a direct correction would be too costly in terms of mass.

For an 800 km orbit, the drift relative to heliosynchronism is given in [10]:

$$\frac{\Delta H}{\Delta J} \text{ (hours per day)} = -7 \times 10^{-3} \Delta i \text{ (degrees)} + 1.4 \times 10^{-5} \Delta r_p \text{ (km)}$$

(the orbit being an elliptical one with an apogee of 800 km).

The first correction simultaneously alters the semimajor axis and the inclination. With the perigee lowered to 300 km, Δr_p equals -500 km, and the associated negative drift term has a value of

$$\frac{\Delta H}{\Delta J} (rp) = -7 \times 10^{-3} \text{ hours/day,}$$

One possible strategy is to transfer into a 300 x 800 orbit by changing inclination, drift for 270 days, and then make the orbit a circular 300 km one while maintaining the inclination at the heliosynchronous value.

$$\begin{aligned} \text{-- First correction: } \Delta r_p &= 500 \text{ km} & \Delta i &= +1.38^\circ \\ & & \Delta V &= 225 \text{ m/sec} \end{aligned}$$

-- Drift for 270 days in a 300 x 800 km orbit, $i = 100^\circ$.

$$\begin{aligned} \text{-- Second correction: } \Delta r_a &= -500 \text{ km} & \Delta i &= -3.4^\circ \\ & & \Delta V &= 460 \text{ m/sec} \end{aligned}$$

/42

The two corrections taken together correspond to a propulsive mass equal to 21% of the initial mass.

It will be necessary to make a deeper analysis of this strategy and to choose between a system of two solid-fuel engines and a liquid fuel system.

3.2.4 Generation of Power

The angle λ between the sun and the normal to the orbit varies between $+17^\circ$ and -30° , according to the season. Thus, eclipses occur in one part of the year ($\lambda > 17^\circ$). This part of the year is centered on one of the solstices. Which one depends on the local time chosen for the node.

The electrical power available from the generating system and originating in the cells glued to one whole side is about 270 to 314 W, according to the season, with a diameter of 2 meters. Depending on the operating cycle adopted for the ionic engine, it is possible that it will be necessary to add a crown of cells around the edge. A crown 25 cm deep will make the available power increase to between 420 and 490 W.

3.2.5 Other Subsystems

The other subsystems do not pose any particular problem provided that a more precise evaluation of the aeriels necessary for the TM-TC-LOC system that takes account of the desired localization accuracy (10 to 100 m) is made.

3.3 Ground Segment

/43

The problems linked to the ground segment are of two orders:

- recovery of the telemetric data stored on board;
- decametric localization of the satellite to permit reduction of the measurements.

The amount of data to transmit per orbit (about 6 Mbits) does not present any obvious problems for the ground stations currently available or for the use of bubble memories.

For reconstructing altitude, the measurement of drag, the use of a model with a large enough potential (see TOPEX study) and of a few laser stations should solve the problem.

3.4 Development Plan

A very preliminary evaluation ended in the following results:

Feasibility Studies (Phase A)

Duration of about 1 1/2 years, end of 1981 to mid 1983.

Essentially concerns:

- Scientific mission: precisely define the scientific missions, simulate the instrument's operation in the adopted configurations, evaluate the system's overall accuracy.
- Instrument: gradiometer feasibility study, limit of resolution, specifications of inflight calibration mechanisms.
- Mission and vehicle: detailed analysis of mission, choice of orbit, orbit acquisition, identification of possible configurations, general architecture of satellite, attitudinal movements and deformations, corrections, stabilization. In principle, the subsystems should not pose any feasibility problems since we are building on equipment that is either already in existence or presently under development (SPOT gyros, Symphonie cold gas system, photo-cell strip star trackers of the ERS 1 type).
- Elaboration of the development plan and evaluation of its cost.

/44

Detailed Design (Phase B)

Duration of about two years, mid 1983 to mid 1985.

During this phase, the plan is to conduct complementary technical studies of SUPERCACTUS and to create functional mockups of the gradiometer and the inflight calibration mechanisms. As far as the system is concerned: detailed study of its functions (attitude control, orbital control, thermal control, electrical generation, data acquisition and transmission, structure, mechanical architecture), detailed design of the satellite, ground stations and data processing, system and subsystem specification, organization of the construction phase, precise determination of costs.

Development and Construction (Phases C and D)

Duration of about 2 1/2 years, mid 1985 to end of 1987.

Customary model fabrication and qualification phase, particularly qualification of SUPERCACTUS and the complete platform, equipped with calibration mechanisms.

The studies in phases A and B have to determine which preliminary models to build ahead of the complete qualification and flight models.

Key Dates

/45

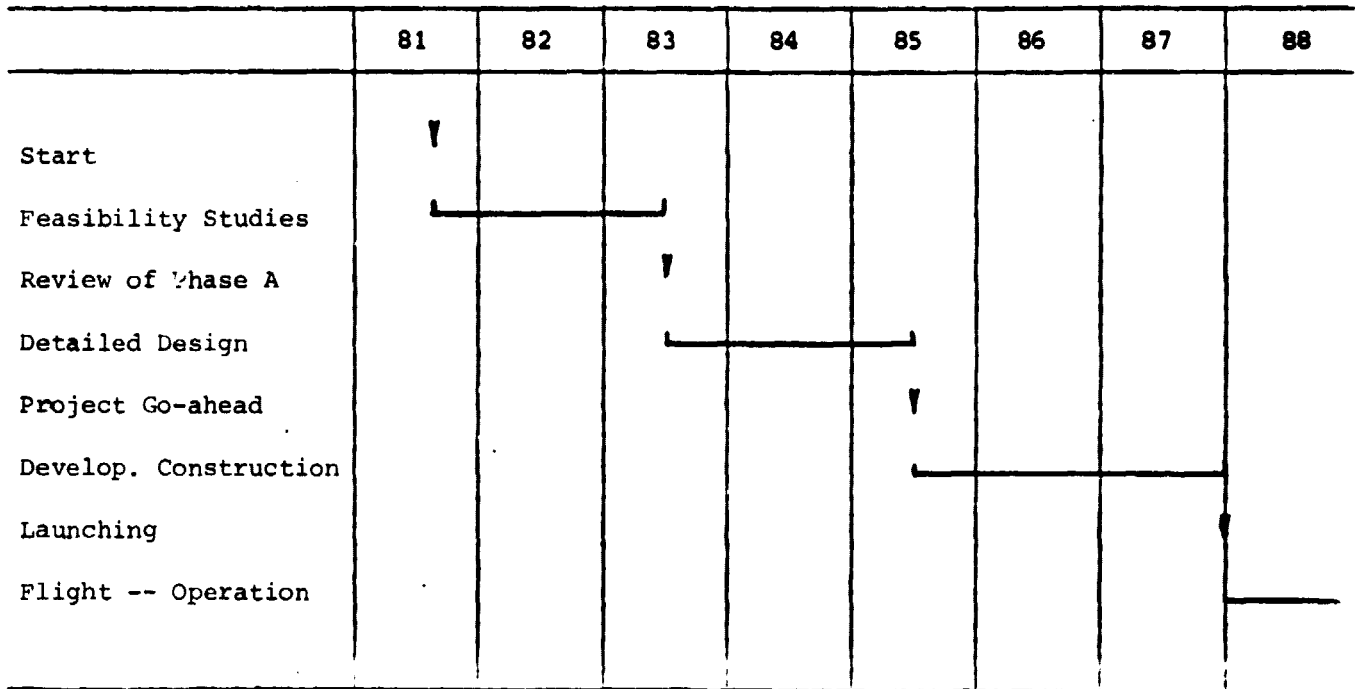
The principal stages might be the following (See chart below):

- End of 1981: Decision to launch phase A.
- Mid 1982: Synthesis of the first feasibility study results (particularly the first simulations) and decision to pursue phase A.
- Mid 1983: Review of phase A and decision to launch phase B.

-- Mid 1985: Review of detailed design and decision to build the project.

-- End of 1987: Launching.

The launching could therefore take place at the end of 1987 or the beginning of 1988. This is not too late, considering that solar activity will reach a maximum in 1991.



3.5 Operation

/46

3.5.1 Measurement Reduction

Among the problems connected to measurement reduction, one merits particular attention because of its possible impact on the satellite's design. The test masses are subjected to both internal gravitation

forces, linked to the satellite (distribution of masses inside the satellite), and external ones (earth, moon, sun). We shall always be analyzing the resultant of these forces. However, the purpose of the mission concerns analyzing the external forces. To separate the effects, one must work in different conditions: reduction of the data obtained at very different altitudes or reduction of data collected with permutations in the role of the satellite's axes. One will therefore consider:

- the advantage to a temporary intermediate orbit, for example at 800 km;
- the advantage to and the necessity of being able to rotate the satellite about itself in order to exchange the axes (as was done with CASTOR).

These problems must be studied with care.

3.5.2 Calculation of Field Anomalies

Any determination of parameters linked to the geopotential at the earth's surface, such as geoid altitude or gravitational anomalies, based on observations made on board a satellite suffers from what the geodesists call the "problem of downward prolongation". This is simply the problem of the attenuation of the signal caused by an anomaly with increasing altitude. It is illustrated by table 2, where we have tabulated the variance of gravitational anomalies (extrapolated beyond an order and degree of 36) for blocks of wavelengths (i.e. between two given degrees ℓ_1 and ℓ_2) as a function of altitude.

We could say, for example, that the signal is considerably amplified in the 73 to 180 block when one descends from 250 km to 0 km, and so is the error in the detected signal, unfortunately. This is the first difficulty (almost nonexistent up to $\ell = 36$, as all the present overall models prove a posteriori) which does not yet

/47

have a satisfactory theoretical solution. However, the smaller the error in the measured components is, the less troublesome it will be. This consideration might justify a (redundant) system to measure the six tensor components. In fact, only fine covariance analyses or very realistic simulations can show the limits in reconstructing the parameters we are interested in. In any case, a first observation made by all the theoreticians is that by measuring the components of $\nabla^2 T$ (where T is the perturbing potential), the propagation of errors is less for the calculation of gravitational anomalies ($\sim ||\nabla T||$) than for T itself, or in other words for tracing the geoid. This difficulty has already been pointed out.

Table 2
 $\sigma (\Delta g; \ell_1 \rightarrow \ell_2)$ in mgals, for Different Altitudes

Spectral Extent $\ell_1 \rightarrow \ell_2$ Altitude (km)	2 → 18	19 → 36	37 → 72	73 → 180
400	8.85	2.35	0.69	0.06
250	10.82	4.25	1.96	0.40
0	15.97	12.44	14.09	17.54

The reconstruction process, for example of gravitational anomalies, raises problems of another nature. The use of spherical harmonics is impracticable because this is not a regionalized representation of the field. Point masses or surface densities could be used, but it is even more preferable to use the generalized Stokes equation, which presents an even more "pointed" regionalization and makes it possible to directly obtain the gravitational anomalies near the subsatellite

trace. In theory, the relationship connecting the (infinite) vector of values of g to the (finite) vector of measurement q is discretized /48 in the form:

where the operator S implicitly contains Pizetti's extension of the core of the Stokes operator. Mathematically, like all inverse problems, this problem is called "improperly stated", and a possible solution consists in carrying out a Tikhonov regularization by looking for solutions \bar{g} such that

where D is the covariance matrix of measurement errors, C_{gg} is the (infinite) covariance matrix of the field g (estimated in steps or extrapolated from what one already knows of the selfcorrelation function of g at the present wavelengths), and α is a regularization factor. The solution has to be judged by its stability in relation to "reasonable" variations in α or perturbations in the matrix C_{gg} .

In any case, it must be recognized that the practical resolution of such a problem requires sophisticated computing apparatus and might involve dividing up the steps of the calculation within Europe, even at the final level. This is similar to what we have already been doing for the last decade with the C. Reigber group in Munich.

4. Conclusion

/49

Significant progress in the knowledge of the gravitational field of the earth and other telluric bodies necessarily passes by way of the development of new measurement techniques, either satellite-to-satellite tracking or gradiometry.

Gradiometry, in essence the simpler of the two, now seems within our ability to perform, and the first analyses, which are performed and briefly presented in this document, show the possibility of occupying an original niche in this field.

The preliminary design is based on a gradiometer with four ONERA microaccelerometers. It calls for an approximately 1,000 kg lens-shaped satellite stabilized in the local orbital frame of reference. Its orbit would be a 6:00-18:00 heliosynchronous one ranging between 200 and 300 km in altitude.

This mission to a large extent uses the French space experience acquired in the D 5B (Castor) and SPOT programs.

In contrast, it appears that we have insufficient knowledge of the spectral nature of gravitation measurements and their possible separation from perturbations, the intrinsic accuracy of the gradiometer's measurements (equalization of scale factors), the accuracy in controlling and reconstructing the vehicle's angular velocity, and the methods of dealing with the data (model creation). These various points do not, at the present stage, bring the first conclusions into question, but they do necessitate complementary studies to confirm the project's feasibility and the ultimate accuracy attainable in the measurement of anomalies in the gravitational field.

REFERENCES

1. Delattre, M., et al. "Les Essais en Orbite de l'Accéléromètre CACTUS," [Orbital Tests of the CACTUS Accelerometer], ONERA Publication No. 1976-5.
2. Bernard, Alain, Michel Gay, Rémy Juillerat, "The Cactus Accelerometer," AGARDograph no. 254, April 1981.
3. Bernard, Alain, et al., "Radiation Pressures Determination with the CACTUS Accelerometer," Paper presented at the 20th Meeting of COSPAR, Tel-Aviv, June 1977.
4. Boudon, Yves, François Barlier, Alain Bernard, Rémy Juillerat, Anne-Marie Mainguy, and Jean-Jacques Walch, "Synthèse des Résultats en vol de l'Accéléromètre CACTUS pour des Accélérations Inférieures à 10^{-9} G," [Summary of Inflight Test Results of the CACTUS Accelerometer for Acceleration of Less than 10^{-9} G], Paper presented at the 29th International Astronautics Congress, Dubrovnik, October 1978.
5. Bernard, Alain, Michel Gay, and Ann-Marie Mainguy, "Super-Cactus: Project of 10^{-11} g Three-Axis Accelerometer," Paper presented at the 30th International Astronautics Congress, Munich, September 1979, (Acta Astronautica, 7, [1980]).
6. Mainguy, Anne-Marie, Jacques Bouttes, Rémy Juillerat, and François Barlier, "Mesure du Bilan Radiatif de la Terre à l'aide d'un Accéléromètre Ultrasensible -- Projet BIRAMIS," [Measurement of the Make-Up of Terrestrial Radiation with the Aid of an Ultra-sensitive Accelerometer -- Project BIRAMIS], Paper presented at the International Conference on "The Evolution of Planetary Atmospheres and Climatology of the Earth" organized by CNES, Nice, October 1978.
7. Mainguy, Anne-Marie, Alain Bernard, Manola Romero, Jacques Bouttes, and François Barlier, "BIRAMIS: Mesure du Bilan Radiatif de la Terre par Microaccélérométrie Spatiale," [BIRAMIS: Measurement of the Make-Up of Terrestrial Radiation by Space Microaccelerometry], Paper presented to the Congress of the Société Française de Physique, Toulouse, June 1979.
8. Runavot, Jean-Jacques, "GRADIO: Analyse de mission," [GRADIO: Mission Analysis], Number 234 PRT/AMP/AP, August 31, 1981.
9. Bouzat, C., Number 81/CT/PRT/SST/SS 277, August 24, 1981.
10. Breton, Jacques and Alain Perret, "Possibilités de manoeuvre au voisinage d'une orbite héliosynchrone," [Maneuvering in the Vicinity of a Heliosynchronous Orbit], Number 43/PRT/AMP/D, February 17, 1981.